

¹²H. Wahlquist, J. Chem. Phys. **35**, 1708 (1961);
 R. Arndt, J. Appl. Phys. **36**, 2522 (1965).
¹³J. L. Hall and C. J. Bordé, Phys. Rev. Lett. **30**,
 1101 (1973).
¹⁴J. T. Hougen, J. Mol. Spectrosc. **46**, 490 (1973);
 K. Uehara and K. Shimoda, J. Phys. Soc. Jpn. **36**, 542

(1974).
¹⁵R. L. Barger, T. C. English, and J. B. West, in
Proceedings of the Twenty-ninth Symposium on Fre-
quency Control, Fort Monmouth, New Jersey, 1975
 (Electronic Industries Association, Washington, D. C.,
 1975), p. 316.

The following Letter should have appeared in the 1 November 1976 issue. We regret that a misunderstanding resulted in publication of reference material instead of the submitted manuscript. See Erratum, this issue, page 1368.

Strong-Signal Theory of a Free-Electron Laser*

F. A. Hopf, P. Meystre, M. O. Scully

Department of Physics and Optical Sciences Center, University of Arizona, Tucson, Arizona 85721

and

W. H. Louisell

Department of Physics, University of Southern California, Los Angeles, California 90007

(Received 13 August 1976)

The strong-signal regime of a free-electron laser is analyzed in terms of a set of "generalized Bloch equations." We show that for current free-electron-laser configurations the saturation will be reached for a field on the order of 10^7 V/m, with an efficiency at saturation of 5×10^{-3} . However, a strong reshaping of the electron distribution may alter the efficiency of free-electron lasers in cases where the electron beam is recycled from one shot to the next.

Recently, a considerable effort has been made toward the realization of a free-electron laser. Elias *et al.*¹ have passed a relativistic electron beam ($E = \gamma mc^2 \approx 24$ MeV) through a helical static magnetic field, and have observed stimulated scattering at $10.6 \mu\text{m}$. On the theoretical side, a number of authors²⁻⁵ have computed the small-signal gain of this laser, and there is now general agreement on the functional form as well as the numerical value of the gain. In order to assess the potential of any practical laser device, it is necessary to *complement* the small-signal theory by an analysis of the mechanisms of saturation. In the present case, we do not need a quantum theory.⁵ In fact, the quantum theory of a free-electron laser is extremely tedious, and neither *desirable* nor necessary.

In this Letter, we present the strong-signal theory of a free-electron laser. Our analysis is completely classical and relies on the coupling of Maxwell's equations to the relativistic collisionless Boltzmann equation.⁵ We use the Weizsacker-Williams approximation,⁶ which allows us to simulate the static magnetic field of period λ_q by a fictitious incident electromagnetic field of wavelength $\lambda_i = (1 + v/c)\lambda_q \approx 2\lambda_q$, propagating in the op-

posite direction of the electron beam. We then express the problem in terms of a set of generalized Bloch equations coupled to Maxwell's equations.

Following the derivation of Ref. 5, we find that the coupled Maxwell-Boltzmann equations can be reduced to the set of equations

$$\left(\frac{\partial^2}{\partial z^2} - \frac{1}{c^2} \frac{\partial^2}{\partial t^2} \right) \bar{A}_T = \frac{e^2 \mathcal{F}}{mc \epsilon_0} \bar{A}_T \int_{-\infty}^{\infty} dp_z \frac{h(z, p_z, t)}{\gamma}, \quad (1)$$

$$\frac{\partial h}{\partial t} + \frac{p_z}{m\gamma} \frac{\partial h}{\partial z} = \frac{e^2}{m\gamma} \frac{\partial}{\partial z} \left(\frac{\bar{A}_T^2}{2} \right) \frac{\partial h}{\partial p_z}. \quad (2)$$

Here, the electrons have been taken to be injected inside the cavity along the z axis. $p_z = \gamma m v_z$ is the z component of the electron momentum, and $\gamma \approx [1 + (p_z/mc)^2]^{1/2}$. The filling factor \mathcal{F} is the ratio of the section πa^2 of the electron beam to the section of the cavity. $h(z, p_z, t)$ is the longitudinal part of the Boltzmann distribution function and is related to the electron number $N(t)$ inside the cavity by

$$N(t) = \pi a^2 \int_{-\infty}^{\infty} dp_z \int_0^L dz h(z, p_z, t), \quad (3)$$

where L is the length of the cavity.

\bar{A}_T is the vector potential that we take to be of

the form

$$\begin{aligned} \vec{A}_T = & \hat{e}_- \{ A_i \exp[-i(\omega_i t + k_i z)] \\ & + A_s(t) \exp[-i(\omega_s t - k_s z)] \}, + c.c., \end{aligned} \quad (4)$$

where i and s refer to the incident and scattered modes, respectively, and

$$\hat{e}_\pm = (\hat{x} \pm i\hat{y})/\sqrt{2}.$$

To obtain the small-signal gain, we expanded $h(z, p_z, t)$ in powers of $|A_i A_s|$, and kept terms only up to first order. It would be tempting to expand to higher orders to compute the saturation, keeping, for example, terms up to third order in the field strength as in the usual procedures of laser theory. However, this perturbative expansion diverges. To approach the strong-signal theory, it is necessary to use some other expansion for $h(z, p_z, t)$, such that each term contains the saturation to all orders in the field.

To this end, we express $h(z, p_z, t)$ as the harmonic expansion

$$\begin{aligned} h(z, p_z, t) = & n(z, p_z, t) \\ & + \sum_{m=1}^{\infty} (i g_m e^{im(\Delta\omega t - Kz)} + c.c.), \end{aligned} \quad (5)$$

where $K = K_i + k_s$ and $\Delta\omega = \omega_s - \omega_i$.

Keeping only terms up to $m=1$ in expansion (5), we find that the Boltzmann equation (2) can be re-expressed as the generalized Bloch equations

$$\partial R_1 / \partial \zeta + \mathcal{O} R_2 = -\partial R_3 / \partial \mathcal{O}, \quad (6a)$$

$$\partial R_2 / \partial \zeta - \mathcal{O} R_1 = 0, \quad (6b)$$

$$\partial R_3 / \partial \zeta = -\partial R_1 / \partial \mathcal{O}, \quad (6c)$$

subject to the boundary conditions

$$\begin{aligned} R_1(0, \mathcal{O}) = R_2(0, \mathcal{O}) = 0, \\ R_3(0, \mathcal{O}) \text{ prescribed by the initial} \\ \text{electron momentum distribution.} \end{aligned} \quad (7)$$

$R_i(\zeta, \mathcal{O})$ are dimensionless functions that are related to n and g_i through

$$R_1 = (mc\sqrt{2}/4n_e\sigma\beta_s\gamma_s)(g_1 + g_1^*), \quad (8a)$$

$$R_2 = -i(mc\sqrt{2}/4n_e\sigma\beta_s\gamma_s)(g_1 - g_1^*), \quad (8b)$$

$$R_3 = (mc/2n_e\sigma\beta_s\gamma_s)n, \quad (8c)$$

where

$$\sigma^2 = mc/4\sqrt{2}\gamma_s^4\beta_s^2e^2A_iA_s, \quad (9)$$

and

$$\beta_s = (1 - 1/\gamma_s^2)^{1/2} = \Delta\omega/Kc. \quad (10)$$

n_e is the electron density inside the cavity when

no field is present. The scaling coefficients serve to eliminate all explicit field dependence from Eqs. (6). The dimensionless variable \mathcal{O} is related to the detuning

$$\mu = \Delta\omega/v_z - K, \quad (11)$$

of the laser cavity from the condition of exact momentum conservation.^{4,5} In the region of interest $-2\pi \leq \mu L \leq 2\pi$, \mathcal{O} can be approximated by the leading term of a Taylor expansion. We express it in terms of a scale length l as

$$\mathcal{O} \simeq -\mu l. \quad (12)$$

The dimensionless length ζ is expressed in terms of the scale length l as

$$\zeta = z/l. \quad (13)$$

We will discuss the meaning of the length $l = mc\gamma_s^2\beta_s/2^{1/4}eK(A_iA_s)^{1/2}$ later. Before doing this, let us note that the set of equations (6) presents a striking resemblance to the optical Bloch equations,⁷ where R_3 would be the population inversion, and R_1 the polarization. However, it differs from them in two respects. First, the signs on the right-hand side of Eqs. (6a) and (6c) are opposite in the optical Bloch equations; and second, the right-hand side of the Bloch equations contains R_3 and R_1 , rather than their derivatives. This difference in structure lies in the fact that in a free-electron laser, the gain is not proportional to the electron distribution function. It is its derivative with respect to p_z (rather than the gain itself) which plays the role of an inversion.⁵

In the small-cavity limit, the gain is then given in terms of the maximum small-signal gain⁵ g_{\max} as

$$\begin{aligned} g(A_i, A_s, p_0, L) \\ = g_{\max}(A_i, p_0, L) \mathfrak{S}(A_i, A_s, p_0, L), \end{aligned} \quad (14)$$

where the saturation function \mathfrak{S} is the double integral

$$\begin{aligned} \mathfrak{S}(A_i, A_s, p_0, L) \\ = \frac{1}{4} \pi^3 (l/L)^3 \int_0^{L/l} d\zeta \int_{-\infty}^{\infty} d\mathcal{O} R_1(\zeta, \mathcal{O}), \end{aligned} \quad (15)$$

where p_0 is the initial electron momentum.

In Fig. 1, we present a numerical computation of the saturation function \mathfrak{S} as a function of μL and $\sqrt{\mathfrak{R}} \equiv (\sqrt{2}/\pi^2)(L/l)^2$. This figure was computed in the experimentally relevant limit in which μL is much larger than the initial width of R_3 ("small-cavity" limit). The vertical axis corresponds to the small-signal regime ($\sqrt{\mathfrak{R}}=0$), and is in agreement with the results of Ref. 5. The working

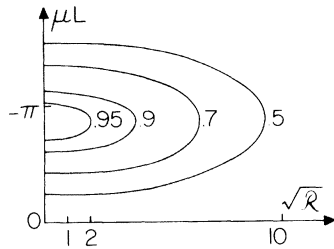


FIG. 1. Plot of the equisaturation curves $s = \text{constant}$ as a function of \sqrt{R} and $-\mu L$. The curves are labeled with their value of $s = 0.95, 0.9, 0.7,$ and 0.5 . These results were obtained in the small cavity limit, and the ratio of the electron momentum distribution width to the cavity bandwidth was taken to be $1/20$.

point of the free-electron laser should be chosen to be about $\mu L = -\pi$, and for this value s reaches the value 0.5 for $\sqrt{R} \approx g$.

The numerical results demonstrate that our scaling coefficient correctly describes the saturation by the requirement $R \sim 1$ or $l \sim L$. We would like to derive l (to within numerical factors) by a heuristic argument that will serve to make connection with the physics of the saturation, using the scaling relations of ordinary lasers.

Let us suppose that the mechanism of saturation is a deceleration of the electrons through the gain line to the point of zero gain. The maximum amount of energy ΔE that a single electron can transfer to the field is

$$\Delta E = (\lambda_s/L) \gamma^3 mc^2, \quad (16)$$

where λ_s is the wavelength of the scattered light. In the limit that the scattered flux S_s becomes large, the gain is limited by the maximum energy flux S_{ex} available from the electron beam per unit time:

$$S_{ex} = (\mathcal{F} n_e c^2 / L) \Delta E. \quad (17)$$

Defining as usual the saturation flux S_{sat} as the ratio of S_{ex} to the maximum small signal gain g_{max} ,

$$S_{sat} = S_{ex} / g_{max}, \quad (18)$$

we find that the scale length l is related to the saturation flux through the relation

$$(\sqrt{2}/\pi^2)(L/l)^2 = (S_s/S_{sat})^{1/2}. \quad (19)$$

The left-hand side of Eq. (19) is precisely the parameter \sqrt{R} used in the numerical computation, and is equal to 1 for $S_s = S_{sat}$. We note that the right-hand side of Eq. (19) is $(S_s/S_{sat})^{1/2}$, rather than S_s/S_{sat} . This is due to the fact that the field

is excited coherently by the electron beam.

It follows that the maximum field extractable from a free-electron laser (i.e., the output field when the laser is in the saturation regime) is

$$A_{s,max} \approx (\lambda_s/L)^2 (mc)^2 \gamma^4 / e^2 A_i. \quad (20)$$

With use of the numerical values of the Stanford experiment, Eq. (20) gives a maximum extractable field on the order of $E_{s,max} \approx 10^7$ V/m (i.e., $S_{sat} \sim 10^7$ W/cm²) for a static magnetic field of 2.4 kG. The efficiency at saturation is $\eta_{sat} = (\lambda_s/L) \gamma^2$ and is on the order of 5×10^{-3} in this case. This implies that free-electron lasers have the potential to work at high power, but they must be operated in a pulsed mode, with small per-shot efficiency. In this context, it is important to assess the possibility of recycling the electron beam from one shot to the next. There would not be any difficulty in doing that if the only mechanism of saturation was an electron deceleration through the gain line, as assumed earlier in this Letter. However, we want to emphasize that although this assumption gives a correct estimate of the saturation, it is by no means the unique way of understanding it. In reality, a more detailed analysis shows that a major contribution to the saturation is a strong alteration of the electron distribution such that the laser eventually reaches the large-cavity limit. This reshaping will be analyzed in detail in a later publication in order to give an estimate of the efficiency of a free-electron laser.

In the present analysis we have considered only the terms up to first harmonics in the expansion of $h(z, p_z, t)$. For each supplementary term kept in Eq. (5), the set of equations (6) is increased by two new equations, and the problem becomes very complicated very fast. We have checked numerically the contribution of the second harmonics, and have found that their effect on the saturation function s was less than 10% for the region of practical interest.

The advantage of the free-electron laser, as compared to other presently existing light sources, lies essentially in the fact that they are in principle tunable continuously over an extremely large spectral range (from the far ir to at least the soft uv), simply by changing the energy of the electron beam. In this Letter, we have demonstrated that they also have the potential to work at high power. Although further efficiency studies will be necessary in order to assess their large-scale applications, free-electron lasers seem at the present time to be an attractive alternative to conventional lasers.

A detailed presentation of these results, as well as analytical solutions for some limiting cases, will be presented elsewhere.

*Work supported by the U. S. Energy Research and Development Administration.

¹L. R. Elias, W. H. Fairbank, J. M. J. Madey, H. A. Schwettmann, and T. J. Smith, *Phys. Rev. Lett.* **36**, 717 (1976).

²R. H. Pantell, G. Soncini, and H. E. Puthoff, *IEEE J.*

Quantum Electron. **4**, 905 (1971).

³J. M. J. Madey, *J. Appl. Phys.* **42**, 1906 (1971); J. M. J. Madey, H. A. Schwettman, and W. M. Fairbank, *IEEE Trans. Nucl. Sci.* **NS-20**, 980 (1973).

⁴V. P. Sukhatme and P. W. Wolff, *J. Appl. Phys.* **44**, 2331 (1973).

⁵F. A. Hopf, P. Meystre, M. O. Scully, and W. H. Louisell, *Opt. Commun.* **18**, 413 (1976).

⁶J. D. Jackson, *Classical Electrodynamics* (Wiley, New York, 1962).

⁷See for instance, L. Allen and J. H. Eberly, *Optical Resonance and Two-Level Atoms* (Wiley-Interscience, New York, 1975).

Experimental Study of Enhanced Diffusion by Electrostatic Fluctuations in an Ohmically Heated Toroidal Plasma

S. M. Hamberger, L. E. Sharp, J. B. Lister, and S. Mrowka*

EURATOM-United Kingdom Atomic Energy Authority Fusion Association, Culham Laboratory, Abingdon, Oxon, OX14 3DB, United Kingdom

(Received 2 August 1976)

The low-frequency density fluctuations observed in an ohmically heated toroidal plasma are found to be consistent with a spectrum of electrostatic drift modes which can account for the measured anomalous particle loss rate.

It is now generally accepted that, at least in low β , long-mean-free-path plasma, there is likely to be a significant contribution to the cross-field transport of toroidally confined plasma due to the presence of low-frequency ($\omega \ll \omega_{ci}$) long-wavelength ($k\lambda_D \ll 1$) electrostatic modes, and experimental studies on tokamaks¹ are just beginning. This contribution can conveniently be expressed² in the form of a diffusion coefficient

$$D_{\perp} \sim \sum_{\vec{k}} \tau(\vec{k})^{-1} [c k_{\perp} \varphi(\vec{k}) / \omega(\vec{k}) B]^2,$$

where $\tau(\vec{k})$ is the correlation time for fluctuations with frequency $\omega(\vec{k})$ and amplitude $\varphi(\vec{k})$. Whatever their origin, these modes will have the nature of drift waves with $k_{\perp} \gg k_{\parallel}$, $\omega \sim \omega^* = k_{\perp} v_D = (k_{\perp} / L_n) \times (cT / eB)$.

The relation between such fluctuations, plasma confinement, and, for example, current density can in principle be studied in any toroidal-confinement experiment; in practice, however, for a tokamak the situation is generally complicated by magnetohydrodynamic (MHD) activity (which causes turbulent effects of a different kind and may confuse the measurements) due to the existence of rational magnetic surfaces, while the plasma parameters in the more elegant conducting ring devices (levitron, multipoles) are usually not typical of larger toroidal devices and the ordering of the magnetic field components is differ-

ent.³

This problem can be largely overcome by using a stellarator with large vacuum rotational transform to define the confining field so that one can vary plasma conditions appreciably with an ohmic heating current either so small that the magnetic configuration, at least to first order, is unchanged, or, where this is not possible, so chosen as to avoid obvious MHD instability. In this Letter, we report the results of some observations using this approach which demonstrates the relationship between plasma confinement, drift-wave-like density fluctuations, and electron-drift/thermal velocity ratio ξ .

The experiment was performed in TORO (described in detail elsewhere⁴) in which closed magnetic surfaces are produced entirely by currents in a single set of unipolar helical windings (the "ultimate torsatron configuration"). The plasma is produced and heated by a longitudinal discharge ($I \sim 1-10$ kA, $1-5$ ms) controlled by making small (approximately a few percent), slow changes in the quasi-steady confining field. Experiments were made with mean fields in the range $4-10$ kG. The plasma boundary was defined only by the magnetic separatrix, with no material limiter or other object in contact with the plasma, and had peak and mean parameters (as indicated by a caret and a bar, respectively) $2 \times 10^{12} \leq \bar{n}$